

PAPER

# Calculation of resonances by analytical continuation: role of asymptotic behavior of coupling function

To cite this article: T Bárta and J Horáek 2020 *Phys. Scr.* **95** 065401

View the [article online](#) for updates and enhancements.

# Calculation of resonances by analytical continuation: role of asymptotic behavior of coupling function

T Bárta and J Horáček 

Faculty of Mathematics and Physics, Charles University, V Holešovičkách 2, 180 00 Prague, Czech Republic

E-mail: [jiho@matfyz.cz](mailto:jiho@matfyz.cz)

Received 30 December 2019, revised 4 February 2020

Accepted for publication 24 February 2020

Published 16 March 2020



CrossMark

## Abstract

The regularized analytical continuation method (RAC) counts among the most powerful modern method for determination of resonance energies and resonance widths of low energy atomic and molecular systems including large systems of biological importance. By this method the resonance state is transformed into bound state by addition of an attractive potential. In this paper the choice of the perturbation potential is discussed and the performance of the method studied using model potential. It is shown that for correct applications of the RAC method the knowledge of the asymptotic behavior of the basic ingredient of the method, the coupling function  $\lambda(\kappa)$ , is important. In this paper we find the correct asymptotic form of  $\lambda(\kappa)$  for broad class of realistic potentials and for nonzero values of angular momentum. New RAC formula convenient for singular perturbation potentials is proposed.

Keywords: atomic resonance, molecular resonance, regularized analytical continuation method (RAC), analytical continuation in coupling constant

(Some figures may appear in colour only in the online journal)

## 1. Introduction

Resonances in non-relativistic quantum mechanics are defined as solutions of the Schrödinger equation

$$-\frac{d^2\psi_l(r)}{dr^2} + \frac{l(l+1)}{r^2}\psi_l(r) + U(r)\psi_l(r) = k^2\psi_l(r) \quad (1)$$

$l = 0, 1, 2, \dots$  satisfying the Siegert boundary conditions [1]

$$\psi_l(0) = 0, \quad \frac{\psi_l'(R)}{\psi_l(R)} = ik, \quad (2)$$

where  $R$  is a distance from the origin at which the interaction  $U(r) = 0$ . It is important to mention that the eigenvalue  $k$  enters the boundary condition equation (2) and thus the problem to find the eigenvalue  $k$  is nonlinear [2]. Generally all the eigenvalues can be divided into three groups [3]:

- $\text{Im } k > 0, \text{ Re } k = 0$ , bound states. These states are easily calculated because the solution  $\psi_l(r) \in L_2$ .

- $\text{Im } k < 0, \text{ Re } k = 0$ , virtual states.
- $\text{Im } k < 0, \text{ Re } k \neq 0$ , resonance states.

Both resonance and virtual states are difficult to calculate because the solution  $\psi_l(r)$  at large distances oscillates and exponentially increases.

Recently the so-called method of regularized analytical continuation [4] was proposed and successfully applied to a resonances formed by collisions of electrons with molecules [5] and atoms [6]. The RAC approach is based on the method of analytical continuation in coupling constant (ACCC) (see for example [3, 5, 7–10]).

It is the purpose of this paper to improve the accuracy and stability of the RAC method by studying the analytical features of the so-called coupling function  $\lambda(\kappa)$  on simple models with the aim to improve its performance when applied to real atomic and molecular systems. Rigorous mathematical proof of its asymptotic behavior is provided for a broad class of potentials for nonzero values of the angular momentum  $l$ .

## 2. RAC method

The essence of the RAC method consists in changing the strength of the potential  $U(r)$

$$U(r) \rightarrow U(r) + \lambda U(r) \quad (3)$$

so that for properly chosen  $\lambda$  the resonances are analytically continued into the bound state region. In the bound state region we have

$$\begin{aligned} -\frac{d^2\psi_l(r)}{dr^2} + \frac{l(l+1)}{r^2}\psi_l(r) + (1+\lambda)U(r)\psi_l(r) \\ = -\frac{\kappa^2}{2}\psi_l(r) \end{aligned} \quad (4)$$

where the energy  $E$  is negative,  $E = \frac{k^2}{2} = -\frac{\kappa^2}{2}$ ,  $k = i\kappa$  and  $\psi_l(r) \in L_2$ . The energy now depends also on the strength parameter  $\lambda$ , i.e.  $\kappa = \kappa(\lambda)$  and similarly we can consider the inverse function  $\lambda = \lambda(\kappa)$ . The resonances are then found by solving the equation

$$\lambda(\kappa) = 0. \quad (5)$$

In real applications it is better to use as the perturbation potential a potential different from  $U(r)$ , i.e.

$$U(r) \rightarrow U(r) + \lambda V(r) \quad (6)$$

and again the resonances are obtained by solving equation (5). The transformation from resonance region to bound state region proceeds as follows: for nonzero angular momentum two symmetric resonance poles located on the unphysical sheet start to move under influence of attractive perturbation potential toward the origin. At some strength of the perturbation both poles reach the origin and coincide. The S-matrix has then a pole of second order at the origin. At further increasing the strength of the attractive perturbation potential one pole moves upwards to the physical sheet and forms a bound state. The other pole moves downwards and forms a virtual state on the unphysical sheet [3].

The lowest RAC approximation, the [3/1] approximation [4], is a ratio of two polynomials,  $P(\kappa)$  and  $Q(\kappa)$ , of the order 3 and 1 respectively,

$$\lambda(\kappa) = \lambda_0 \frac{(\kappa^2 + 2\alpha^2\kappa + \omega)(1 + \delta^2\kappa)}{\omega + \kappa(2\alpha^2 + \delta^2\omega)}, \quad \omega = \alpha^4 + \beta^2. \quad (7)$$

This function has two complex conjugate zeros

$$\kappa_{1,2} = -\alpha^2 \pm i\beta.$$

or in  $k$ -space

$$k_{1,2} = \pm\beta - i\alpha^2$$

and obviously describes one pair of resonances with the energy  $E = (\beta^2 - \alpha^4)/2$  and width  $\Gamma = 2\alpha^2\beta$ . The parameters  $\alpha$  and  $\beta$  have direct physical meaning determining the real and imaginary parts of the resonance energy. The

parameter  $\delta$  describes a virtual state with energy  $E_V = -\frac{\delta^4}{2}$ . To get the resonance parameters this function has to be fitted to the input data. The standard way is to minimize the functional

$$\chi^2 = \frac{1}{N} \sum_{i=1}^N |\lambda(\kappa_i) - \lambda_i|^2. \quad (8)$$

where  $N$  is the number of bound state energies  $\{E_i = -\frac{\kappa_i^2}{2}\}$  computed with the perturbation  $\lambda_i V(r)$ .

The resonance parameters are obtained by minimizing a nonlinear function  $\chi^2$  which is a function of several variables. Minimization of a nonlinear function in several variables is a difficult problem. The weakest point of this procedure is to find the starting point (initial values of all variables) for a larger number of variables. A bad choice may lead to a local minima. In all real cases the resonance energy and width may be approximately estimated. To use their approximate position the RAC formula was designed such that it contains directly these parameters as fitting parameters. A second advantage of the RAC approach is the special form of the function  $\lambda(\kappa)$ , equation (7). It is designed in such a way that the resonance pairs are always located on the unphysical sheet, for details see [4].

In the following we will show that the asymptotic behavior of the function  $\lambda(\kappa)$  is of essential importance for efficient performance of the RAC method. In this study we use two types of perturbation potentials:

1. The Gauss potential

$$V(r) = -e^{-ar^2}, \quad (9)$$

and

2. the attenuated Coulomb potential

$$V(r) = -\frac{e^{-ar^2}}{r}. \quad (10)$$

The Gauss potential is finite everywhere whereas the attenuated Coulomb potential equation (10) is singular at the origin. In the following we will show that this difference is essential for the analytical continuation. Both potentials were discussed recently by White *et al* [11]. In addition to the attenuated Coulomb and Gauss potential they considered also pure Coulomb potential. They conclude that the results with the attenuated Coulomb potential are slightly better than those obtained with the Coulomb potential and significantly better than those obtained with the Gauss potential.

## 3. Asymptotic behavior of the coupling function

The problem of asymptotic behavior of the coupling function  $\lambda(\kappa)$  for finite potentials has been studied by Freitas and Krejčířík [12] with the result that  $\lambda(\kappa)$  increases as  $\kappa^2$  at  $\kappa \rightarrow \infty$ . In this paper we provide an alternative proof of this statement and in addition prove that for potential singular at the origin, as the attenuated Coulomb potential equation (10),

this is no longer true. We prove that in such a case the coupling function  $\lambda(\kappa)$  increases only linearly  $\lambda(\kappa) \approx \kappa$  for  $\kappa \rightarrow \infty$ . In addition we show that the correct account of the asymptotic behavior is of great importance for efficient performance of the RAC method.

3.1. Proof

This part contains exact formulation and proofs of the main results on the asymptotic behavior of the coupling function  $\lambda(\kappa)$ . Let us consider equation (4) where we write  $t$  instead of  $r$  (we work in polar coordinates below and using  $r$  would be confusing) and  $-V$  instead of  $U$ . So, we rewrite equation (4) as

$$\begin{aligned} \psi''(t) &= A(t)\psi(t), \\ A(t) &= \frac{l(l+1)}{t^2} + \kappa^2 - \lambda V(t). \end{aligned} \tag{11}$$

We are interested in solutions  $\psi$  that satisfy the boundary conditions

$$\lim_{t \rightarrow 0+} \psi(t) = 0 = \lim_{t \rightarrow +\infty} \psi(t) \tag{12}$$

If  $l$  and  $V$  are fixed, then for any  $\kappa \in \mathbb{R}$  we denote

$$\begin{aligned} \Lambda(\kappa) &= \{ \lambda \geq 0 : \exists \psi \in C^2((0, +\infty)), \\ &\psi \neq 0 \text{ and satisfying (11) and (12)} \} \end{aligned}$$

and

$$\lambda(\kappa) = \inf \Lambda(\kappa) \quad (\text{with } \lambda(\kappa) = +\infty \text{ if } \Lambda(\kappa) \text{ is empty}).$$

Let us formulate the following technical assumptions

(A) There exists  $n \in \mathbb{N}$  such that for every  $\kappa, \lambda > 0$  the function  $A: (0, +\infty) \rightarrow \mathbb{R}$  defined in equation (11) has at most  $n$  roots.

$$(V) \lim_{t \rightarrow +\infty} V(t) = 0, \int_1^{+\infty} |V(t)| dt < +\infty.$$

Let us mention that these assumptions are satisfied for  $ce^{-at^2}$  and  $\frac{c}{t}e^{-at^2}$ , so the theorems below apply to the Gauss and attenuated Coulomb potentials.

**Theorem 1 (Bounded potential).** *Let  $l \in (0, +\infty)$  and let  $V: [0, +\infty) \rightarrow \mathbb{R}$  be a continuous function such that (A) and (V) hold. Denote  $C_0 = \frac{1}{m_0}$ , where  $m_0 = \max_{t \geq 0} V(t) > 0$ . Then for every  $C_1 > C_0$  there exists  $\kappa_0 > 0$  such that*

$$C_0 \kappa^2 \leq \lambda(\kappa) \leq C_1 \kappa^2 \tag{13}$$

holds for every  $\kappa > \kappa_0$ .

**Theorem 2 (Unbounded potential).** *Let  $l \in (0, +\infty)$  and let  $U: [0, +\infty) \rightarrow \mathbb{R}$  be a continuous bounded function such that  $V(t) = \frac{1}{t}U(t)$  satisfies (V) and (A). Assume that  $U(0) > 0$  and denote  $C_0 = \frac{2\sqrt{l(l+1)}}{U(0)}$ . Then there exists  $C_1 > C_0$  and  $\kappa_0 > 0$  such that*

$$C_0 \kappa \leq \lambda(\kappa) \leq C_1 \kappa \tag{14}$$

holds for every  $\kappa > \kappa_0$ .

To prove these theorems, let us first consider the following general problem

$$\psi''(t) = (B(t) - \lambda V(t))\psi(t) \tag{15}$$

and denote as above

$$\begin{aligned} \Lambda &= \{ \lambda \geq 0 : \exists \psi \in C^2((0, +\infty)), \\ &\psi \neq 0 \text{ satisfying (15) and (12)} \} \end{aligned}$$

and

$$L = \inf \Lambda \quad (\text{with } L = +\infty \text{ if } \Lambda \text{ is empty}).$$

Let us assume that potentials  $B$  and  $V$  satisfy the following.

$$(B) \lim_{t \rightarrow 0+} B(t)t^2 = B_0 \in (0, +\infty), \lim_{t \rightarrow +\infty} B(t) = B_\infty \in (0, +\infty), \int_0^1 B(t)t - \frac{B_0}{t} < +\infty, \int_1^{+\infty} B(t) - B_\infty < +\infty.$$

$$(BV) 0 = \lim_{t \rightarrow +\infty} \frac{V(t)}{B(t)}. \text{ There exists } n \in \mathbb{N} \text{ such that for all } \lambda > 0 \text{ the function } B(t) + \lambda V(t) \text{ has at most } n \text{ roots in } (0, +\infty).$$

**Lemma 3.** *Let (B), (V), (BV) holds. Assume that there exist  $\bar{\lambda}, \underline{\lambda} > 0$  such that*

- (i)  $B(t) + \lambda V(t) \geq 0$  for all  $\lambda \in (0, \underline{\lambda}), t > 0$  and
- (ii) there exist  $\omega > 0$  such that  $B(t) + \bar{\lambda} V(t) < -\omega^2$  on an interval  $[a, b] \subset (0, +\infty)$ , where  $b - a = \frac{2\pi n}{\omega}$ .

Then

$$\underline{\lambda} \leq L \leq \bar{\lambda}.$$

**Proof. Step 1.** We first observe that for every  $\lambda \in \mathbb{R}$  the solutions  $\psi$  with  $\lim_{t \rightarrow +\infty} \psi(t) = 0$  form a space of dimension 1 and the same is true for solutions satisfying  $\lim_{t \rightarrow 0+} \psi(t) = 0$ . In fact, for  $+\infty$  it follows immediately from [13, corollary XI.9.2] since  $\lim_{t \rightarrow +\infty} B(t) + \lambda V(t) = B_\infty = \mu^2$  and  $\int^{+\infty} q(t)dt = \int^{+\infty} B(t) - B_\infty + \lambda|V(t)|dt < +\infty$ . At zero, the statement follows by the same corollary after substitution  $u(s) = e^{\frac{1}{2}s}\psi(e^{-s})$  which transforms problem equation (15) at 0+ to

$$u''(s) = \left( B(e^{-s})e^{-2s} + \frac{1}{4} + \lambda V(e^{-s})e^{-2s} \right) u(s) \tag{16}$$

at  $+\infty$ . Here the corollary applies with  $\mu^2 = \lim_{s \rightarrow +\infty} B(e^{-s})e^{-2s} + \frac{1}{4} + \lambda V(e^{-s})e^{-2s} = B_0 + \frac{1}{4}$  and  $q(s) = B(e^{-s})e^{-2s} + \lambda V(e^{-s})e^{-2s} - B_0$ . We have

$$\int_1^{+\infty} q(s)ds = \int_0^{1/e} B(t)t + \lambda V(t)t - \frac{B_0}{t} dt < +\infty.$$

**Step 2.** Let  $a, b$  and  $\omega$  be as in assumption (ii). For a fixed  $\lambda$  let us denote  $\psi_\infty$ , resp.  $\psi_0$  solutions to equation (15) satisfying

$$1 = \lim_{t \rightarrow +\infty} e^{\mu_\infty t} \psi_\infty(t) \text{ with } \mu_\infty = \sqrt{B_\infty},$$

resp.

$$1 = \lim_{s \rightarrow +\infty} e^{\mu_0 s} u(s) = \lim_{s \rightarrow +\infty} e^{\mu_0 s} e^{\frac{1}{2}s} \psi_0(e^{-s})$$

with  $\mu_0 = \sqrt{B_0 + \frac{1}{4}}$ .

Such solutions exist, are unique, and depend continuously on  $\lambda$  (see [13, section X.4]). For a function  $y \in C^1(I)$  we introduce  $\omega$ -polar coordinates  $(\rho, \phi): I \rightarrow \mathbb{R}^2$  as functions satisfying

$$y(t) = \rho(t) \cos \phi(t), \quad y'(t) = \omega \rho(t) \sin \phi(t).$$

In particular, if  $\phi_0$ , resp.  $\phi_\infty$  are the  $\omega$ -angles of solutions  $\psi_0$ , resp.  $\psi_\infty$ , then  $\phi_0(\tau)$ ,  $\phi_\infty(\tau)$  depend continuously on  $\lambda$  for any  $\tau \in (0, +\infty)$ .

**Step 3.** Observe that if  $A(t) < 0$  on an interval  $I$ , then the angle  $\phi(t)$  in  $\omega$ -polar coordinates of a solution  $\psi(t)$  of  $\psi'' = A(t)\psi$  is decreasing on  $I$ . If  $A(t) > 0$  on  $I$ , then the solution is either positive and convex or negative and concave, which implies that its  $\omega$ -angle  $\phi(t)$  may increase at most by  $\pi$  (if, e.g., a solution is positive and decreasing (and convex) on a part of  $I$ , then it may be positive and increasing on another part of  $I$  or negative and decreasing, but not both, so its angle stays in an interval of length  $\pi$ ).

Since  $\lim_{t \rightarrow 0+} \frac{V(t)}{B(t)} = 0 = \lim_{t \rightarrow +\infty} \frac{V(t)}{B(t)}$  and  $B_0, B_\infty > 0$ , there exist  $c, d \in (0, +\infty)$ ,  $c < d$  such that  $B(t) + \lambda V(t) > 0$  on  $(0, c) \cup (d, +\infty)$  for all  $\lambda \leq \bar{\lambda}$ . For  $\lambda = \bar{\lambda}$  we have  $A(t) \geq 0$  on  $\mathbb{R}_+$ , therefore the solutions  $\psi_0, \psi_\infty$  defined in Step 2 satisfy  $\phi_0(d) \in (0, \pi/2)$  ( $\psi_0$  is positive, and therefore convex and increasing),  $\phi_\infty(d) \in (-\pi/2, 0)$  ( $\psi_\infty$  is positive, and therefore convex and decreasing). Hence,  $\phi_0(d) - \phi_\infty(d) > 0$  for  $\lambda = \bar{\lambda}$ .

It remains to show the opposite inequality

$$\phi_0(d) - \phi_\infty(d) \leq 0 \text{ for } \lambda = \bar{\lambda}. \tag{17}$$

Then, since the values  $\phi_0(d), \phi_\infty(d)$  change continuously with  $\lambda$  (by Step 2), there exists  $\lambda \in [\underline{\lambda}, \bar{\lambda}]$  for which  $\phi_0(d) - \phi_\infty(d) = 0$ , which means  $\psi_0 \equiv c\psi_\infty$  on  $\mathbb{R}_+$ , i.e.,  $\lambda \in \Lambda$  and the lemma is proved.

We show equation (17). Since,  $B(t) + \lambda V(t) > 0$  on  $(d, +\infty)$  for all  $\lambda \in [\underline{\lambda}, \bar{\lambda}]$ , the solution on  $(d, +\infty)$  is for every  $\lambda$  positive decreasing convex, so  $\phi_\infty(d) \in (-\pi/2, 0)$  for all  $\lambda \in [\underline{\lambda}, \bar{\lambda}]$ . Analogously,  $\phi_0(c) \in (0, \pi/2)$  for all  $\lambda \in [\underline{\lambda}, \bar{\lambda}]$ . Let  $\lambda = \bar{\lambda}$ . On the interval  $[c, d]$ , the function  $B(t) + \lambda V(t)$  has at most  $n$  zeros. It means that there are at most  $n$  subintervals, where  $B(t) + \lambda V(t)$  is positive, so  $\phi_0$  may increase by at most  $n\pi$  on these intervals. On the remaining subintervals  $B(t) + \lambda V(t)$  is negative, so  $\phi_0$  is decreasing and, moreover, on the interval  $[a, b]$  where  $A(t) < -\omega^2$  we have  $\phi_0(a) - \phi_0(b) > 2n\pi$  by the Sturm comparison theorem (see e.g. [13, theorem X.3.1 and its proof]). It follows that  $\phi_0(d) < \pi/2 + n\pi - 2n\pi < \pi/2 - n\pi$ . Therefore  $\phi_0(d) - \phi_\infty(d) < \pi - n\pi \leq 0$ . This completes the proof.  $\square$

**Proof of theorem 1.** We can see that for  $B(t) = \frac{l(l+1)}{t^2} + \kappa^2$  and  $V(t)$  the assumptions (B), (V), (BV) are satisfied for every  $\kappa > 0$ . Let  $\kappa \in \mathbb{R}$  be fixed. Then obviously, assumption (i) of

lemma 3 holds with  $\underline{\lambda} = \kappa^2 C_0$ . Now, let us take  $m \in (0, m_0)$  arbitrarily. By continuity of  $V$  there is an interval  $[a, b] \subset (0, +\infty)$  where  $V(t) > m$ . Set

$$\bar{\lambda}(\kappa) = \frac{1}{m} \left( \frac{l(l+1)}{a^2} + \kappa^2 + \omega^2 \right), \quad \omega = \frac{2\pi n}{b-a}.$$

Then for  $\lambda \geq \bar{\lambda}(\kappa)$  and all  $t \in [a, b]$  we have

$$A(t) = \frac{l(l+1)}{t^2} + \kappa^2 - \lambda V(t) < \frac{l(l+1)}{a^2} + \kappa^2 - \bar{\lambda}(\kappa)m = -\omega^2.$$

So, by lemma 3 we have

$$C_0 \kappa^2 \leq \lambda(\kappa) \leq \frac{1}{m} \left( \frac{l(l+1)}{a^2} + \kappa^2 + \omega^2 \right) = \kappa^2 \frac{1}{m} \left( 1 + \frac{l(l+1) + a^2 \omega^2}{ma^2 \kappa^2} \right).$$

Let  $C_1 > C_0 = \frac{1}{m_0}$ . Then we can choose  $m \in (0, m_0)$  such that  $\frac{1}{m} < C_1$ . Since  $a$  and  $\omega$  depend on  $m$  only, there exists  $\kappa_0$  such that for all  $\kappa \geq \kappa_0$  we have

$$\frac{1}{m} \left( 1 + \frac{l(l+1) + a^2 \omega^2}{ma^2 \kappa^2} \right) < C_1$$

and the proof is complete.  $\square$

**Proof of theorem 2.** First of all, we can see that for  $B(t) = \frac{l(l+1)}{t^2} + \kappa^2$  and  $V(t)$  the assumptions (B), (V), (BV) are satisfied for every  $\kappa > 0$ . Let us write

$$A(t) = \frac{1}{t^2} (l(l+1) + \kappa^2 t^2 - \lambda U(t)t) = \frac{1}{t^2} \left( \left( \kappa t - \frac{\lambda U(t)}{2\kappa} \right)^2 + l(l+1) - \frac{\lambda^2 U(t)^2}{4\kappa^2} \right)$$

and we can see that  $A(t) > 0$  on  $(0, +\infty)$  provided

$$\lambda < \frac{2\sqrt{l(l+1)}}{\max U(t)} \kappa =: \underline{\lambda}.$$

So,  $\underline{\lambda}$  satisfies condition (i) of lemma 3. We show that for an appropriate constant  $C_1$  the number  $\bar{\lambda} = C_1 \kappa$  satisfies condition (i) for all sufficiently large  $\kappa$ . Let  $C_1$  be a fixed constant (its value is specified below), then for any  $\kappa$  we set  $\bar{\lambda} = C_1 \kappa$  and

$$\tau = \frac{2l(l+1)}{\bar{\lambda}U(0)} = \frac{2l(l+1)}{C_1 \kappa U(0)}.$$

Then for any positive  $c$

$$A(c\tau) = \frac{l(l+1)}{(c\tau)^2} + \kappa^2 - \frac{\bar{\lambda}U(c\tau)}{c\tau} = \frac{l(l+1)}{(c\tau)^2} \left( 1 - \frac{cU(c\tau)}{U(0)} \right) + \kappa^2 - l(l+1) \frac{U(c\tau)}{c\tau^2 U(0)}.$$

Let  $D > 0$  be so large that

$$\frac{D}{\sqrt{D+2}} \geq \frac{3\pi n}{\sqrt{l(l+1)}}$$

and  $\kappa$  be so large (therefore  $\tau$  so small) that

$\frac{1}{2}U(0) \leq U(t) \leq 2U(0)$  for all  $t \in [0, (D + 2)\tau]$ . Then

$$\frac{cU(c\tau)}{U(0)} \geq 1 \quad \text{for all } c \in [2, (D + 2)].$$

Hence, for  $c \in [2, (D + 2)]$  we have

$$\begin{aligned} A(c\tau) &\leq \kappa^2 - l(l + 1) \frac{U(c\tau)}{c\tau^2 U(0)} \leq \kappa^2 - \frac{l(l + 1)}{2(D + 2)\tau^2} \\ &= \kappa^2 - \frac{U(0)^2 C_1^2}{8l(l + 1)(D + 2)} \kappa^2 \end{aligned}$$

i.e.,

$$A(c\tau) \leq -C_1^2 \kappa^2 \left( \frac{U(0)^2}{8l(l + 1)(D + 2)} - \frac{1}{C_1^2} \right).$$

Then for  $C_1$  large enough, in particular for  $C_1^2 \geq \frac{72l(l + 1)(D + 2)}{U(0)^2}$  we have

$$\begin{aligned} A(t) &\leq -C_1^2 \kappa^2 \frac{U(0)^2}{9l(l + 1)(D + 2)} \\ &= - \left( \frac{C_1 \kappa U(0)}{3\sqrt{(D + 2)}\sqrt{l(l + 1)}} \right)^2 = -\omega^2 \end{aligned}$$

for  $t \in [2\tau, (D + 2)\tau]$ , i.e. on an interval of length

$$D\tau = \frac{2l(l + 1)D}{C_1 \kappa U(0)} \geq \frac{2l(l + 1)}{C_1 \kappa U(0)} \cdot \frac{3\pi n \sqrt{D + 2}}{\sqrt{l(l + 1)}} = \frac{2\pi n}{\omega}.$$

So, condition (ii) of lemma 3 is verified and the proof is complete.  $\square$

#### 4. Model example

To show the importance of the proved results we apply the RAC method to potential scattering problems for which exact results are easily obtainable. As a typical example we can choose the interaction in the form of the Gauss potential

$$U(r) = -U_0 e^{-qr^2}. \quad (18)$$

This potential has been used many times in nuclear physics as a potential model in the theory of nucleon-nucleon scattering, see for example [14]. In this contribution we will consider two examples.

1. Potential with parameters  $U_0 = -5.72$  a.u. and  $q = 0.99$  a.u. supports a p-wave resonance state with energy  $E_R = 0.037012654$  a.u. and width  $\Gamma = 0.020862435$  a.u. In electronvolts this corresponds to  $E_R = 1.0072$  eV and  $\Gamma = 0.5677$  eV (here we use the conversion ratio 1.0 a.u. = 27.211385 eV). These parameters simulate a typical electron molecule p-wave resonance, see for example [4].
2. As a second example we consider a resonance generated by the potential equation (18) with parameters  $U_0 = -0.64$  a.u. and  $q = 0.12$  a.u. The resonance energy  $E_R = 0.3028$  eV and the width  $\Gamma = 0.2989$  eV. This resonance is broad and very close

**Table 1.** Example 1—molecular resonance. Resonance energy  $E_R$  (eV) and the resonance width  $\Gamma$  (eV) calculated at the RAC [3/1] level, equation (7), using the attenuated potential equation (10) as perturbation with  $a = 0.9$ . In the left column the maximal bound states energy used in the fit is indicated. The last column shows the  $\chi^2$  of the fit equation (8).

Max. energy (eV)	$E_R$ (eV)	$\Gamma$ (eV)	$\chi^2$
0.611	1.013	0.603	0.154E-10
0.898	1.010	0.607	0.615E-10
1.515	1.006	0.613	0.356E-09
2.186	1.001	0.617	0.114E-08
2.539	0.999	0.619	0.180E-08
3.281	0.995	0.622	0.390E-08
3.669	0.993	0.623	0.543E-08
4.068	0.991	0.624	0.734E-08
4.899	0.987	0.626	0.125E-07
5.330	0.985	0.626	0.159E-07
5.772	0.983	0.627	0.199E-07
Exact	1.0072	0.5677	

to the elastic threshold. It may be regarded as a model for the  $2s^2\epsilon p \ ^2P^0$  state of beryllium, [15]. Calculation of this type of resonances is a very difficult task.

Let us start with the [3/1] RAC approximation, equation (7), which represents a good compromise between accuracy and the stability of the analytical continuation process and which was applied to many real atomic and molecular resonances. As a first test we take the Example 1 and perturb the model potential with the attenuated Coulomb potential equation (10). The calculation was performed with the potential  $V(r) = -e^{-0.9r^2}/r$ . The perturbed bound state energies were calculated in the range 0.0–6.0 eV. The function  $\lambda$  was fitted using data in the range  $(0 - E_M)$  with increasing maximal energy  $E_M < 6.0$  eV. The results of the fit are collected in table 1. In the left column the maximal bound state energy used for the fit is shown. The resonance energies are in the second column and the widths in the third. From results collected in this table we can make two conclusions:

The resonance energy as well as the width depend on the maximal bound state energy used in the fit. The calculated resonance energy decreases by 30 meV and the width increases by 24 meV from the lowest to the highest energy. This is to be expected because all RAC formulas represent essentially a low-energy approach.

The second observation is that the resonance width is determined with a considerable error. The average resonance energy over the energy range equals 0.998 eV and the width 0.615 eV compared with the exact values 1.007 eV and 0.568 eV.

This is to be compared with the calculation where the perturbing potential was the Gauss type  $V(r) = -e^{-0.9r^2}$ . The results are in table 2. Both resonance energy as well as the width are much more stable at changing the energy extent of the input data. In addition the resonance energy and mainly the width are much more accurate. The Gaussian potential performs in this case much better than attenuated Coulomb potential.

**Table 2.** Example 1—molecular resonance. Resonance energy  $E_R$  (eV) and the resonance width  $\Gamma$  (eV) calculated at the RAC [3/1] level using the Gauss potential equation (9) as perturbation with  $a = 0.9$ . In the left column the maximal bound state energy used in the fit is indicated. The last column shows the  $\chi^2$  of the fit equation (8).

Max. energy (eV)	$E_R$ (eV)	$\Gamma$ (eV)	$\chi^2$
1.098	1.009	0.573	0.108E-16
1.340	1.009	0.574	0.116E-15
1.844	1.009	0.575	0.206E-14
2.371	1.009	0.575	0.124E-13
2.920	1.008	0.576	0.445E-13
3.488	1.008	0.577	0.117E-12
3.779	1.008	0.577	0.175E-12
4.075	1.008	0.577	0.250E-12
4.678	1.008	0.577	0.466E-12
5.298	1.007	0.578	0.781E-12
5.614	1.007	0.578	0.980E-12
Exact	1.0072	0.5677	

**Table 3.** Example 2. The atomic resonance: Resonance energy  $E_R$  (eV) and the resonance width  $\Gamma$  (eV) calculated at the RAC [3/1] level using the attenuated potential equation (10) as perturbation with  $a = 0.1$ .

Max. energy (eV)	$E_R$ (eV)	$\Gamma$ (eV)	$\chi^2$
0.5922	0.3017	0.3199	0.227E-09
0.9328	0.2993	0.3210	0.919E-09
1.5253	0.2961	0.3218	0.379E-08
1.9724	0.2940	0.3219	0.776E-08
2.4604	0.2920	0.3219	0.142E-07
2.9887	0.2899	0.3217	0.241E-07
3.8560	0.2869	0.3211	0.475E-07
4.4840	0.2848	0.3206	0.708E-07
4.8129	0.2837	0.3202	0.853E-07
5.1517	0.2827	0.3199	0.102E-06
5.8591	0.2806	0.3191	0.142E-06
Exact	0.3028	0.2989	

The quality of the both fits is shown in the last column where  $\chi^2$  is printed against the maximal energy used in the fit. It is seen that the  $\chi^2$  of the fit with the Gauss potential is smaller by several orders of magnitude than that obtained with the attenuated Coulomb potential.

For the second example—the atomic resonance we obtain similar results. See tables 3 and 4. Again here the fit with the Gauss potential is much better than that obtained with the attenuated Coulomb perturbation potential. The reason why it is so is hidden in the asymptotic behavior of  $\lambda(\kappa)$ . The RAC [3/1] approximation, equation (7), for which the Gauss perturbation works excellently, behaves as quadratic function at large  $\kappa$  and thus cannot fit well function which increase only linearly with  $\kappa$  as is the case of the attenuated Coulomb potential. The only possibility to comply with the correct asymptotic behavior is set  $\delta$  to zero. In such a case there are only three free parameters and the quality of the fit deteriorates. To remedy this problem we propose for

**Table 4.** Example 2. The atomic resonance: Resonance energy  $E_R$  (eV) and resonance width  $\Gamma$  (eV) calculated at the RAC [3/1] level, using the Gauss potential equation (9) as perturbation with  $a = 0.1$ . In the left column the maximal bound state energy used in the fit is indicated. The last column shows the  $\chi^2$  of the fit equation (8).

Max. energy (eV)	$E_R$ (eV)	$\Gamma$ (eV)	$\chi^2$
0.7789	0.3049	0.3001	0.744E-15
1.5248	0.3051	0.2999	0.419E-13
2.3619	0.3055	0.2992	0.870E-12
2.8082	0.3057	0.2988	0.229E-11
3.7480	0.3064	0.2981	0.960E-11
4.2388	0.3067	0.2977	0.167E-10
4.7423	0.3071	0.2974	0.270E-10
5.2574	0.3075	0.2971	0.412E-10
5.7835	0.3079	0.2967	0.600E-10
6.8659	0.3088	0.2962	0.114E-09
Exact	0.3028	0.2989	

**Table 5.** Example 1—the molecular resonance. Resonance energy  $E_R$  (eV) and resonance width  $\Gamma$  (eV) calculated at the RAC [3/2] level, equation (19), using the attenuated Coulomb potential equation (10) as perturbation with  $a = 0.9$ . In the left column the maximal bound state energy used in the fit is indicated. The last column shows the  $\chi^2$  of the fit equation (8).

Max. energy (eV)	$E_R$ (eV)	$\Gamma$ (eV)	$\chi^2$
0.9718	1.0077	0.5669	0.249E-16
1.2771	1.0079	0.5671	0.901E-16
1.9283	1.0082	0.5675	0.671E-15
2.2729	1.0083	0.5677	0.164E-14
2.9977	1.0085	0.5682	0.725E-14
3.3773	1.0086	0.5686	0.140E-13
3.7681	1.0087	0.5689	0.249E-13
4.1699	1.0088	0.5692	0.414E-13
4.5824	1.0089	0.5696	0.656E-13
5.0057	1.0089	0.5700	0.101E-12
5.8835	1.0090	0.5707	0.217E-12
6.8026	1.0091	0.5715	0.421E-12
Exact	1.0072	0.5677	

singular potential the following RAC formula

$$\lambda^{[3/2]}(\kappa) = \lambda_0 \frac{(\kappa^2 + 2\alpha^2\kappa + \omega)(1 + \delta^2\kappa)}{\omega + \kappa(2\alpha^2 + \delta^2\omega) + \tau\kappa^2}. \quad (19)$$

This function contains five parameters:  $\alpha$ ,  $\beta$ ,  $\delta$ ,  $\lambda_0$  as in the previous case and an additional parameter  $\tau$ . It is obvious that for nonzero  $\tau$  and  $\delta$  this function has a linear asymptote.

The results of the application of this [3/2] formula are in table 5 for the molecular case and in table 6 for the atomic case. Both resonance energies and widths are now much more accurate and are of similar accuracy as the [3/1] results obtained with the Gauss potential.

In figures 1 and 2 we plot the position of the complex eigenvalues of equations (1) with the boundary condition equation (2) for both cases. Figure 1 treats the molecular resonance (example 1) and figure 2 the atomic case (example 2). As already mentioned the eigenvalues depend on the maximal

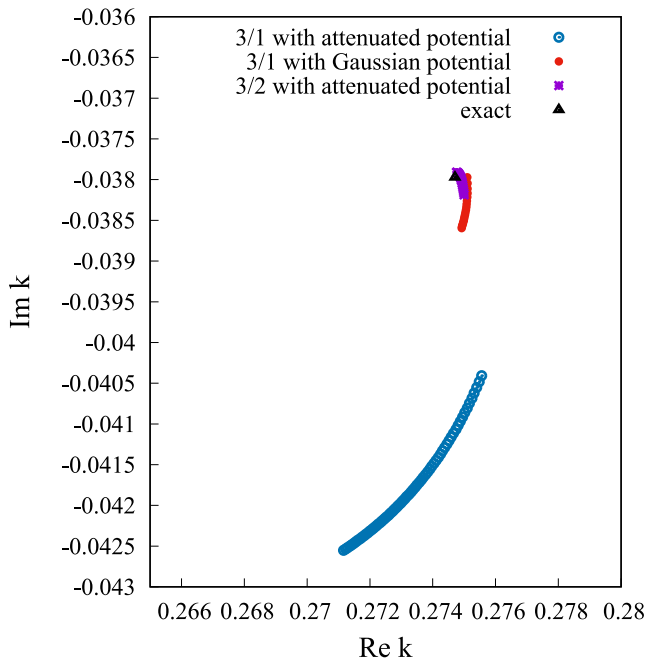


**Figure 1.** Example 1—molecular case. Distribution of S-matrix poles,  $(\text{Re}(k))$  and  $\text{Im}(k)$  in atomic units), defined by equations (1) and (2). Blue circles indicate the [3/1] results obtained with the attenuated Coulomb potential, red circles the same obtained with the Gauss potential for a set of maximal energies in the RAC fit. The results indicated by violet crosses follow from the use of the new [3/2] RAC formula, equation (19) with the attenuated Coulomb potential. The black triangle shows the exact position.

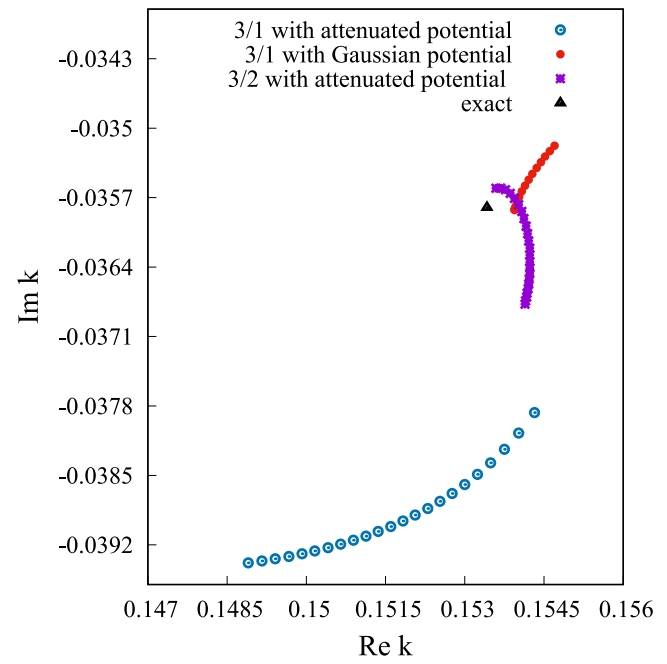


**Figure 2.** Example 2—molecular case. Distribution of S-matrix poles,  $(\text{Re}(k))$  and  $\text{Im}(k)$ , defined by equations (1) and (2). Blue circles indicate the [3/1] results obtained with the attenuated Coulomb potential, red circles the same obtained with the Gauss potential for a set of maximal energies in the RAC fit. The results indicated by violet crosses follow from the use of [3/2] RAC formula, equation (19) with the attenuated potential. The black triangle shows the exact position.

**Table 6.** Example 2: the atomic resonance. Resonance energy  $E_R$  (eV) and the resonance width  $\Gamma$  (eV) calculated at the RAC [3/2] level using the attenuated Coulomb potential equation (10) as perturbation with  $a = 0.1$ . In the left column the maximal bound state energy used in the fit is indicated. The last column shows the  $\chi^2$  of the fit equation (8).

Max. energy (eV)	$E_R$ (eV)	$\Gamma$ (eV)	$\chi^2$
0.7569	0.3048	0.2986	0.964E-14
0.9328	0.3051	0.2992	0.295E-13
1.3172	0.3055	0.3005	0.159E-12
1.7437	0.3057	0.3019	0.538E-12
2.4604	0.3058	0.3039	0.201E-11
2.9887	0.3057	0.3051	0.386E-11
3.2678	0.3056	0.3056	0.511E-11
4.1650	0.3053	0.3069	0.102E-10
4.4840	0.3052	0.3073	0.123E-10
4.8129	0.3051	0.3076	0.146E-10
5.1517	0.3050	0.3079	0.171E-10
5.8591	0.3048	0.3085	0.225E-10
Exact	0.3028	0.2962	

energy used in the fit. In figure 1 the results obtained with the attenuated Coulomb potential and [3/1] RAC formula are denoted by blue circles and the exact position by the black triangle. It is clearly seen that the blue circles, (attenuated potential results), are located far from the exact value and are extended in a considerable region. The [3/1] RAC Gauss results are plotted with red circles. They are much closer to the exact

value than that of the attenuated potential and are confined to a much smaller region. Finally the violet crosses denote results obtained with the [3/2] formula equation (19) and the attenuated Coulomb potential. In figure 2 the results are plotted for the atomic case with the same notation. It is seen that the RAC [3/2] results obtained with the attenuated Coulomb potential are of similar accuracy as those obtained with the RAC [3/1] approximation and Gauss potential.

## 5. Conclusions

In this paper we discussed how the shape of the perturbation potential used for the analytical continuation from bound states to resonance states affects the performance of the RAC method. Two types of perturbation potentials were used both of which were already applied to real problems: 1. The Gauss potential which is finite everywhere (see for example [6]) and the attenuated Coulomb potential singular at the origin discussed recently by White *et al* [11]. The main conclusion from this work is that role of asymptotic behavior of the coupling function  $\lambda(\kappa)$  is important. Rigorous proof is provided that the coupling function  $\lambda(\kappa)$  increases quadratically at large energies for finite potentials whereas it increases only linearly at large energies for singular potentials. A new [3/2] RAC formula was proposed useful for singular potentials. Two examples, one simulating a molecular resonance and one simulating an atomic resonance were presented. It was shown



that for both cases accurate resonance energy and width may be obtained provided correct RAC formula is used: RAC [3/1], equation (7), for finite potentials and RAC [3/2], equation (19), for singular potentials.

In this contribution we restricted ourselves to a simple problem: determination of resonances in potential scattering. To solve this problem efficient numerical techniques exist, see for example [16]. The real power of the RAC method consists in the fact that it can be easily transferred to big atomic and molecular systems as discussed in the Introduction. We hope that results obtained in this study are applicable to the calculation of resonances in real atomic and molecular systems and may substantially improve the efficiency of the RAC method.

### Acknowledgments

This work was supported by the grant agency of the Czech Republic GAČR No. 19-20524S.

### ORCID iDs

J Horáček  <https://orcid.org/0000-0002-4798-4962>

### References

- [1] Siegert A J F 1939 *Phys. Rev.* **56** 750
- [2] Tolstikhin O I, Ostrovsky V N and Nakamura H 1997 *Phys. Rev. Lett.* **79** 2026
- [3] Kukulin V I, Krasnopolsky V M and Horáček J 1988 *Theory of Resonances: Principles and Applications* (Dordrecht/Boston/London: Kluwer Academic Publishers)
- [4] Horáček J, Paidarová I and Čurík R 2015 *J. Chem. Phys.* **143** 184102
- [5] Čurík R, Paidarová I and Horáček J 2016 *EPJD* **70** 146
- [6] Čurík R, Paidarová I and Horáček J 2018 *Phys. Rev. A* **97** 052704
- [7] Horáček J, Mach P and Urban J 2010 *Phys. Rev. A* **82** 032713
- [8] Papp P, Matejčík Š, Mach P, Urban J, Paidarová I and Horáček J 2013 *Chem. Phys.* **418** 8
- [9] Horáček J, Paidarová I and Čurík R 2014 *J. Phys. Chem.* **A118** 6536
- [10] Horáček J 2019 *Phys. Rev. A* **100** 032709
- [11] White A F, Head-Gordon M and McCurdy C W 2017 *J. Chem. Phys.* **146** 044112
- [12] Freitas P and Krejčířík D 2005 *J. Diff Eq.* **211** 168
- [13] Hartman P 1982 *Ordinary Differential Equations, Reprint of the Second Edition* (Boston: Birkhäuser)
- [14] Brown G E and Jackosn A D 1976 *The Nucleon-Nucleon Interaction* (Amsterdam: North-Holland)
- [15] Buckman S J and Clark C W 1994 *Rev. Mod. Phys.* **66** 539
- [16] Ramos A G C P and Iserles A 2015 *Numer. Math.* **131** 541